Electron donating properties of humic acids in saltmarsh soils reflect soil geochemical characteristics

Carlo Bravo [a,b], Rosanna Toniolo [a], Elisa Pellegrini [a,*], Christian Millo [c], Stefano Covelli [d], Marco Contin [a], Ladislau Martin-Neto [e], Maria De Nobili [a]

[a] Department of Agricultural Food Environmental and Animal Sciences, University of Udine, Via Delle Scienze 206, 33100 Udine, Italy
[b] Department of Life Sciences, University of Trieste, Via Licio Giorgieri 5, 34128 Trieste, Italy
[c] Instituto Oceanográfico, University of São Paulo, Praça do Oceanográfico 191, 05508-120 São Paulo, Brazil
[d] Department of Mathematics and Geosciences, University of Trieste, Via Weiss 2, 34128 Trieste, Italy
[e] Embrapa Instrumentação Agropecuária, CP 741, 13560-970 São Carlos, SP, Brazil

ARTICLE INFO

Handling Editor: Matthew Tighe

Keywords:
Humic substances
Salt marshes
Redox
EDC
ABTS

ABSTRACT

In saltmarsh soils, humic acids (HA) are involved in geochemically important redox processes. The electron donating capacity (EDC) of HA depends on their molecular structure, but also reflects the intensity of biological reduction in tidal environments. We examined twelve soils in three saltmarshes located along a geographical gradient and applied a specific sequential extraction procedure for the isolation of HA fractions bound (BHA) or not (FHA) to the mineral matrix by Ca^{2+} bridges, and investigated the relationships of their properties, in particular their EDC, with the biogeochemical characteristics of the soils. Spectroscopic assessment was carried out by UV–vis, FTIR and ^{13}C NMR, quantification and characterization of radicals was performed by electron paramagnetic resonance (EPR) spectroscopy. The EDC was determined by using the 2,2′-azinobis-(3-ethylbenzothiazolinesulfonic acid) (ABTS) decolorization assay and experimental data were fitted to a biphasic model to calculate the contributions of the fast and slow reactions to electron transfer. The results confirmed that the two HA fractions possess different structural characteristics and that BHA present higher EDC values compared to FHA. The EDC of both fractions is strongly related to the geochemical characteristics of soils, and represents an easily measured and highly informative parameter to understand mechanisms affecting redox processes in transitional environments.

1. Introduction

Natural saltmarshes are among the most productive ecosystems of the Earth (Mitsch and Hernandez, 2013) and are important interfaces between terrestrial and marine environments, playing a key role in the global carbon (C) cycle (Chmura et al., 2003). In hydromorphic soils of tidal environments, C cycling and the accumulation of soil organic matter (SOM) are closely related to soil redox conditions, which depend on the length of average daily submergence time (hydroperiod) and the intensity of biological activity (Rabenhorst and Needelman, 2016).

Humic acids (HA), the major refractory components of SOM (Stevenson, 1982), are increasingly being recognized to play many crucial active roles in saltmarshes, regulating geochemical fluxes of elements from land to sea (Steinberg, 2013). Humic acids are redox active SOM components that can be reduced by facultative anaerobic bacteria, which use them as terminal electron acceptors during anaerobic respiration (Keller et al., 2009; Klüpflel et al., 2014; Lovley et al., 1996). They act as electron shuttles, passing on electrons to iron oxides favoring their reductive dissolution and, therefore, regulating the iron cycle (Bauer and Kappler, 2009; Voelker et al., 1997). Humic acids also mediate electron transfer to organic (e.g., halogenated hydrocarbons) and inorganic (e.g., As, Hg) pollutants (Kappler and Haderlein, 2003).

In saltmarsh soils, the redox state of HA is relevant to geochemical redox processes (Valenzuela et al., 2019) and can be conveniently described by their electron donating capacity (EDC), defined as the capacity of a unit weight of a mixture of compounds to donate electrons. The EDC can provide information on the degree of involvement of HA in bacterial anaerobic respiration and in determining the buffering capacity of soils towards redox changes caused by fluctuating water levels and tides, but so far has never been systematically considered in

* Corresponding author.
E-mail address: elisa.pellegrini@uniud.it (E. Pellegrini).

Accepted 5 April 2022

environmental studies.

The EDC of HA depends mainly on the structural presence of phenolic and quinone groups, which act as major reducible moieties (Senesi and Steelink, 1989; Nurmi and Tratnyek, 2002; Ratasuk and Nanny, 2007; Struyk and Sposito, 2001) and varies with their origin (Aeschbacher et al., 2012; Ferreira et al., 2013). Many polyphenols display oxidation reactions that do not allow the measurement of a proper endpoint and pose difficulties in the electrochemical or spectrophotometric determination of their EDC. A recent kinetic study has allowed the validation of the applicability of the 2,2′-azinobis-(3-ethylbenzothiazolinesulfonic acid) (ABTS) decolorization assay to determine the EDC of HA under environmentally meaningful conditions (Bravo et al., 2022), highlighting the concomitant occurrence of a fast and a slow electron transfer mechanisms.

Soil HA are commonly extracted using 0.5 M sodium hydroxide (NaOH) solutions, which solubilizes HA by causing the ionization of acidic functional groups, thereby increasing their molecular polarity and solubility. However, even concentrated NaOH solutions cannot solubilize HA when these are bound to mineral surfaces by cationic bridges. Conversely, alkaline pyrophosphate ($Na_4P_2O_7$) solutions are able to destabilize the Ca^{2+} bridges and extract this fraction (De Nobili et al., 2008). A subsequent extraction with this mildly chelating agent allows the isolation of a fraction of HA possessing different environmental characteristics (Olk, 2006; Olk et al., 2019).

The HA extracted by NaOH (herewith called free HA, FHA) are less physically protected by the mineral phase of the soil, reflecting more recent and local inputs of organic matter. On the other hand, HA extracted by $Na_4P_2O_7$ solutions (herewith called bound HA, BHA), are attached to solid mineral surfaces and may be eventually transported by river water together with the suspended silt and clay particles to which they are adsorbed. In a previous work, Bravo et al. (2020) demonstrated that in lagoon sediments in equilibrium with calcium carbonate ($CaCO_3$) saturated waters, BHA display stronger and conservative terrestrial characteristics (e.g., higher aromaticity) compared to the FHA.

In this work we examined the redox and geochemical properties of FHA and BHA extracted from saltmarsh soils located at different elevation above the mean sea level (a.m.s.l.) and at different distances from the open sea. The aims of this study were to quantify the EDC of HA in saltmarshes in order to: (i) study how the EDC of HA of soils under similar submergence regimes may be affected by their chemo-physical properties and (ii) investigate the relationships of HA and their EDC with the geochemical characteristics and micromorphology of saltmarsh soils. To achieve our goal, we characterized HA with ^{13}C NMR, FTIR and EPR spectroscopy. We also determined the EDC of HA at acidic and neutral pH by using the ABTS decolorization assay and analyzed the kinetics of electron transfer with a biphasic model.

2. Material and methods

2.1. Study area and soil sampling

The Marano and Grado Lagoon (Italy) is located in the northern part of the Adriatic Sea. It extends for 35 km from the Tagliamento to the Isonzo River mouths, with an average width of 5 km covering a total area of ~ 160 km^2. Tides are semi-diurnal, with a mean range of 0.65 m and spring and neap ranges of 1.05 m and 0.22 m. For a detailed

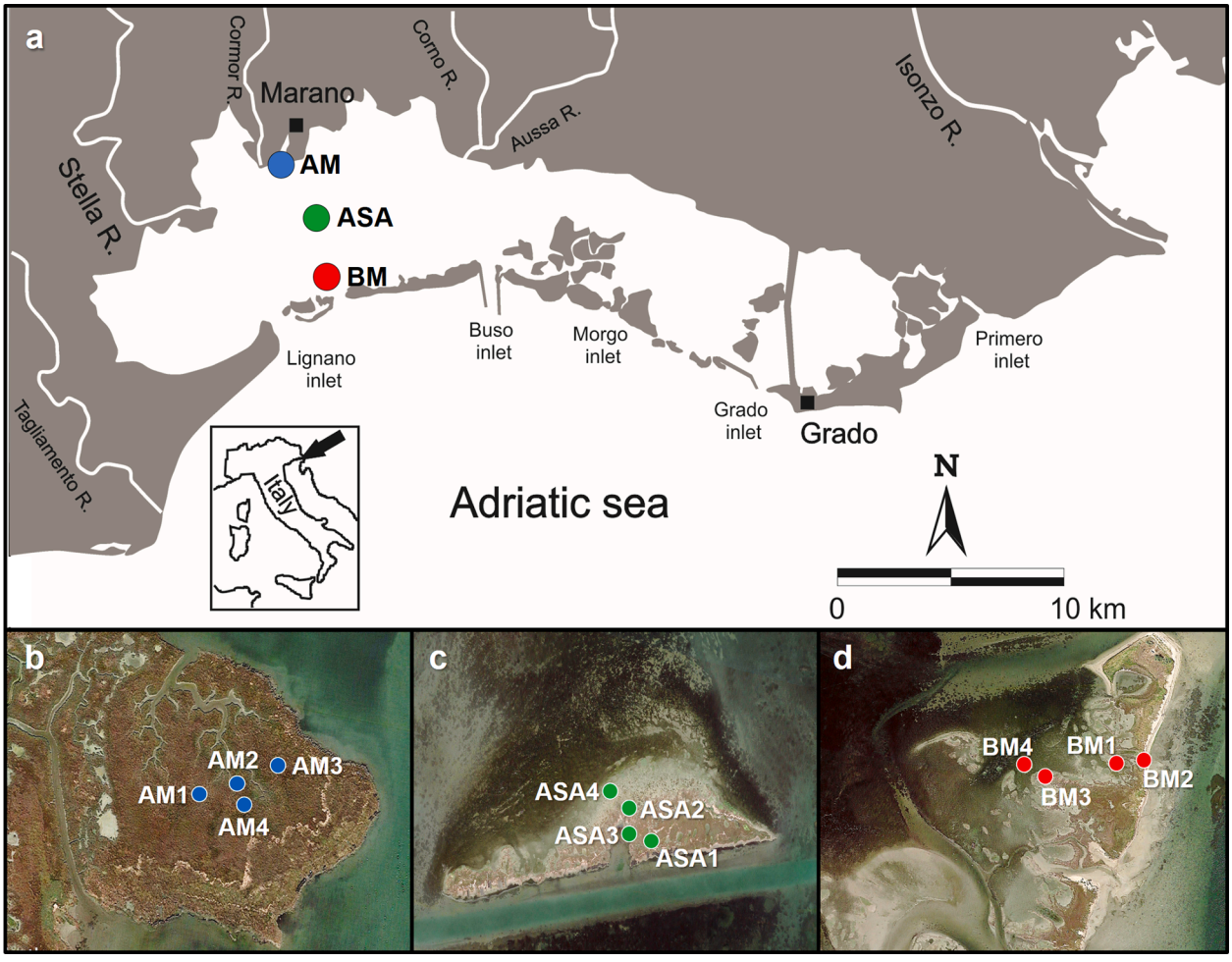

Fig. 1. Geographical location of the Marano and Grado Lagoon, of the three examined saltmarshes (**a**) and of the sampled soils within each saltmarsh (**b-d**).

description of the lagoon and its saltmarshes, the reader may refer to Fontolan et al. (2012).

Three saltmarshes located in the western sector of the lagoon (Fig. 1a) were considered in this study: 1) a high saltmarsh known as Allacciante di Marano (AM), which fringes the mainland and receives significant freshwater inputs from nearby river estuaries; 2) a low saltmarsh called Allacciante di San Andrea (ASA), located in the central part of the lagoon; 3) a back-barrier saltmarsh named Barena di Martignano (BM), with a dominant marine input. Within each saltmarsh, four sampling points were chosen (Fig. 1b-d), following a transect with decreasing elevation above the mean sea level. Geographical coordinates and the dominant plant species of the sampling points are reported in Table S1 (Supporting Information).

At each sampling point, three undisturbed soil cores (diameter 12 cm, depth 20 cm) were collected in PVC tubes. Both ends of the tubes were immediately sealed to preserve the soil water content and avoid contact with air. Cores were transported to the laboratory within a few hours. Here, the upper 2–10 cm of each core (corresponding to the A horizon, where accumulation of organic matter and HA occurs) were separated and pH and redox potential (E_h) measurements were immediately carried out under nitrogen atmosphere. The sampling was carried out in summer (May-July), during low tides within semi-diurnal tide periods.

2.2. Analysis of soils

Soil pH and E_h were measured in 1:2.5 soil/water suspensions using a Basic 20 (Crison) pH-meter after calibrating the pH and Pt electrodes with appropriate standard solutions. Soil texture (percentage of sand, silt and clay) was determined by the hydrometer method (Bouyoucos, 1962).

Total organic carbon (C_{org}) and total nitrogen (N_{tot}) contents of bulk soils and extracted HA were determined using an Elemental Analyzer (Costech Instruments Elemental Combustion System). Carbonates were removed by reaction with 1 M HCl (Nieuwenhuize et al., 1994). Carbon stable isotope compositions of SOM ($\delta^{13}C_{SOM}$) and HA fractions ($\delta^{13}C_{HA}$) were measured with an Isotope Ratio Mass Spectrometer (Thermo Scientific Delta V Advantage) coupled with an Elemental Analyzer (Costech Instruments Elemental Combustion System). Caffeine IAEA 600 and L-glutamic acid USGS 40 were used as certified reference materials for the calibration of raw $\delta^{13}C$ values. Calibrated $\delta^{13}C$ values are expressed in parts per mil (‰) versus the international reference Vienna-Pee Dee Belemnite (V-PDB).

All solutions used in the analyses were prepared using high purity water (18 MΩ resistivity, Milli-Q Corp.).

2.3. Extraction and characterization of HA

Extraction of HA was carried out under N_2 flux, first with 0.5 M NaOH (free HA, FHA) for 1 h and then with 0.1 M $Na_4P_2O_7$ plus 0.1 M NaOH (bound HA, BHA) for another hour (De Nobili et al., 2008). Soil extracts were centrifuged (14000 rpm for 20 min) and supernatants were filtered using 0.2 μm cellulose filters. Free and bound HA were precipitated at pH 1 with 6 M HCl, separated by centrifugation, dialyzed against ultrapure water (until Cl^- free), frozen and then freeze-dried.

UV–vis spectra of HA were recorded after dissolving HA in phosphate buffer (0.1 M, pH 7.0) using a Cary Varian Spectrophotometer in 1 cm quartz cuvettes over a wavelength interval from 220 to 700 nm at a scan rate 60 nm min^{-1}.

The Fourier-transform infrared (FTIR) spectra of the fully protonated acid form of freeze-dried HA were recorded with a FT-IR Spectrum 100 (PerkinElmer) spectrometer equipped with a universal ATR (attenuated total reflectance) sampling device containing a diamond/ZnSe crystal. The spectra were recorded at room temperature in transmission mode over a wavenumber interval from 4000 to 500 cm^{-1} (64 scans at a resolution of 4 cm^{-1}), and are reported in the figures in absorbance units. A background spectrum of air was scanned under the same instrumental conditions before each series of measurements.

The solid-state cross-polarization magic angle spinning (CPMAS) carbon-13 nuclear magnetic resonance (^{13}C NMR) spectra of HA were obtained with an Advance III HD (Bruker) spectrometer operating at 400 MHz. HA samples were packed into a zirconium oxide rotor (5-mm internal diameter). Other instrumental parameters were: contact time 1 ms, delay time 1 s, spinning speed of 10 KHz and 8192 scans for each sample. The structural assignment of different chemical shift regions was performed according to Knicker and Lüdemann (1995). Therefore, each spectrum was divided into the following regions: alkyl C (0–45 ppm), N-alkyl/methoxyl C (45–60 ppm), O-alkyl C (60–110 ppm), aromatic C (110–160 ppm), carboxyl and peptide carbonyl C (160–185 ppm) and carbonyl C (185–245 ppm). The relative ^{13}C intensity distribution was quantified by integration of each chemical shift region.

The electron paramagnetic resonance (EPR) spectra were measured using a Bruker EMX EPR spectrometer operating at the X-band (9.5 GHz). About 40 mg of sample (equivalent to approx. 10 mm in height) were placed in a 3.5 mm quartz tube. Each sample was analyzed at room temperature in triplicate. Other instrumental parameters were: center field 3410 G, sweep width 160 G, sweep time 60 s, microwave power 0.2 mW, modulation amplitude 1 G, and receiver gain 10^4. The number of scans varied from 1 to 9 as a function of the signal to noise ratio of each sample. The microwave power of 0.2 mW was chosen after performing the power saturation curve in one representative sample (Fig. S1). Quantification of the semiquinone-type free radical (SFR) was performed by the secondary standard method, using Cr(III)MgO (g = 1.9797) as a paramagnetic marker (permanently placed in the resonance cavity) calibrated with strong pitch reference (Bruker) of known free radical content (Martin-Neto et al., 2001). The SFR content is given in spins $g_{HA}^{-1} \times 10^{17}$. To calculate areas, linewidth (ΔH) and the spectroscopic splitting factor (g), the spectra were simulated using a double Lorentzian fit.

The fast and slow electron donating capacity (EDC_{fast} and EDC_{slow}, respectively) of HA were determined at pH 4.8 (0.1 M citrate buffer) and pH 7.0 (0.1 M phosphate buffer) using the ABTS decolorization assay, as described in Bravo et al. (2022). A detailed description of the procedure is reported in Text S1.

2.4. Statistics

All measurements were made in triplicate and reported in tables and figures as mean value ± standard deviation of the mean (SD). Differences between treatments were considered significant at $p < 0.05$. Regression analysis, test of significance of the correlation coefficient, and analysis of parallelism were carried out using the software R (Miller and Miller, 2010). Data were then investigated using heat maps in R studio ("gplots" package, R version 4.0.3). Euclidean distances and the complete linkage method were applied for the hierarchical clustering of variables. Variables were previously scaled using the Z-score function: within each variable, values were normalized by subtracting the mean and dividing by the standard deviation.

3. Results

3.1. Soil and soil organic matter characteristics

The examined samples cover a complete range of textural classes spanning from sandy to clayey soils (Fig. S2); their chemo-physical characteristics are summarized in Table S1. The soils of the saltmarsh located nearer to the mainland (AM) present the highest content of finest mineral particles, with mud (silt plus clay) contents ranging from 60 to 70 % and a mean clay content of 40 ± 7 %. In the central saltmarsh (ASA), soil texture is more homogeneous and all samples are classified as loamy sandy clay soils (mean silt and clay contents of 17 ± 3 and 26 ± 4 %, respectively). The soils of the outer saltmarsh (BM) present a

prevalence of coarsest particles (mean sand content of 77 ± 12 %) and the sand content reaches up to 91 % in the BM1 soil.

In all saltmarshes, because of the accumulation of carbonatic silty and sandy particles, the soil pH range is restricted and varies from neutral to weakly alkaline (mean value of 7.5 ± 0.3), with no significant differences among saltmarshes. Indeed, the $CaCO_3$ content is relatively high in all soils and increases from the AM (mean value of 34.1 ± 1.5 %) towards the BM (mean value of 68.7 ± 14.5 %) saltmarsh. Intermediate contents are found in soils of the ASA saltmarsh (mean value of 43.7 ± 1.6 %).

The three saltmarshes are subject to regular inundation during high tides: yearly average daily hydroperiod (calculated according to Pellegrini et al. 2019) is inversely correlated to soil elevation ($R^2 = 0.99$, $p < 0.001$; Fig. S3). As a consequence, soil redox conditions vary from suboxic ($E_h = 88 \pm 12$ mV in AM2) to strongly anoxic ($E_h = -367 \pm 36$ mV in ASA4). Soil E_h values correlate positively with soil elevation ($R^2 = 0.60$, $p < 0.01$) and, albeit not significantly, with clay and C_{org} contents (Fig. S4).

The amount of C_{org} in soils decreases from the AM (mean value of 50.7 ± 6.6 mg g^{-1}) towards the BM (mean value of 6.2 ± 1.9 mg g^{-1}) saltmarsh, likely reflecting the positive effect of physical protection linked to a higher content of clay on C sequestration in soil ($R^2 = 0.80$, $p < 0.001$; Fig. S5a and Table S1). The C_{org} correlates with soil total nitrogen (N_{tot}), yielding a C/N ratio of 12 ($R^2 = 0.99$, $p < 0.001$; Fig. S5b). However, SOM is well differentiated along the geochemical gradient, with less negative $\delta^{13}C$ values and lower C/N ratios towards the sea. The ^{13}C depletion is stronger in the AM saltmarsh (mean value of $\delta^{13}C$ = -25.2 ± 0.3 ‰) with values typical of terrestrial SOM (-Xia et al., 2020) and is coupled to a higher average C/N (11.6 ± 0.5). This reflects both the geographical gradient, i.e. more terrestrial-derived organic C in AM, and the absence of plant communities dominated by C4 plants, which are instead present in the other saltmarshes (ASA4 and BM3 sampling points). The SOM of the outmost saltmarsh BM has a mean value of $\delta^{13}C$ = -21.7 ± 2.2 ‰, whereas the average C/N ratio decreases to 8.3 ± 0.9 and, unlike the other two saltmarshes, SOM C/N values are strongly correlated to $\delta^{13}C$ ($R^2 = 0.96$, $p < 0.001$). Contrary to what could have been expected (Duarte et al., 2018), the gradual increase in $\delta^{13}C$ of SOM registered from the AM towards the BM saltmarsh does not simply reflect changes in the isotopic composition of C inputs from the dominant plant cover of soils. In fact, soils with the same vegetation cover but belonging to different saltmarshes, such as AM3 and ASA2 (both under *Sarcocornia fruticosa*) or AM4 and ASA (both under *Puccinellia festuciformis*), display significantly different isotopic values ($\delta^{13}C$ values of −24.8 ± 0.2 ‰ vs. 18.9 ± 0.2 ‰ and −25.3 ± 0.2 ‰ vs. −21.4 ± 0.3 ‰, respectively). The observed differences can be explained with an increase in C inputs of marine origin (algae and sea weeds) during storms in the outer saltmarsh. This hypothesis is coherent with the decreasing trend of the SOM C/N ratios along the geographical gradient.

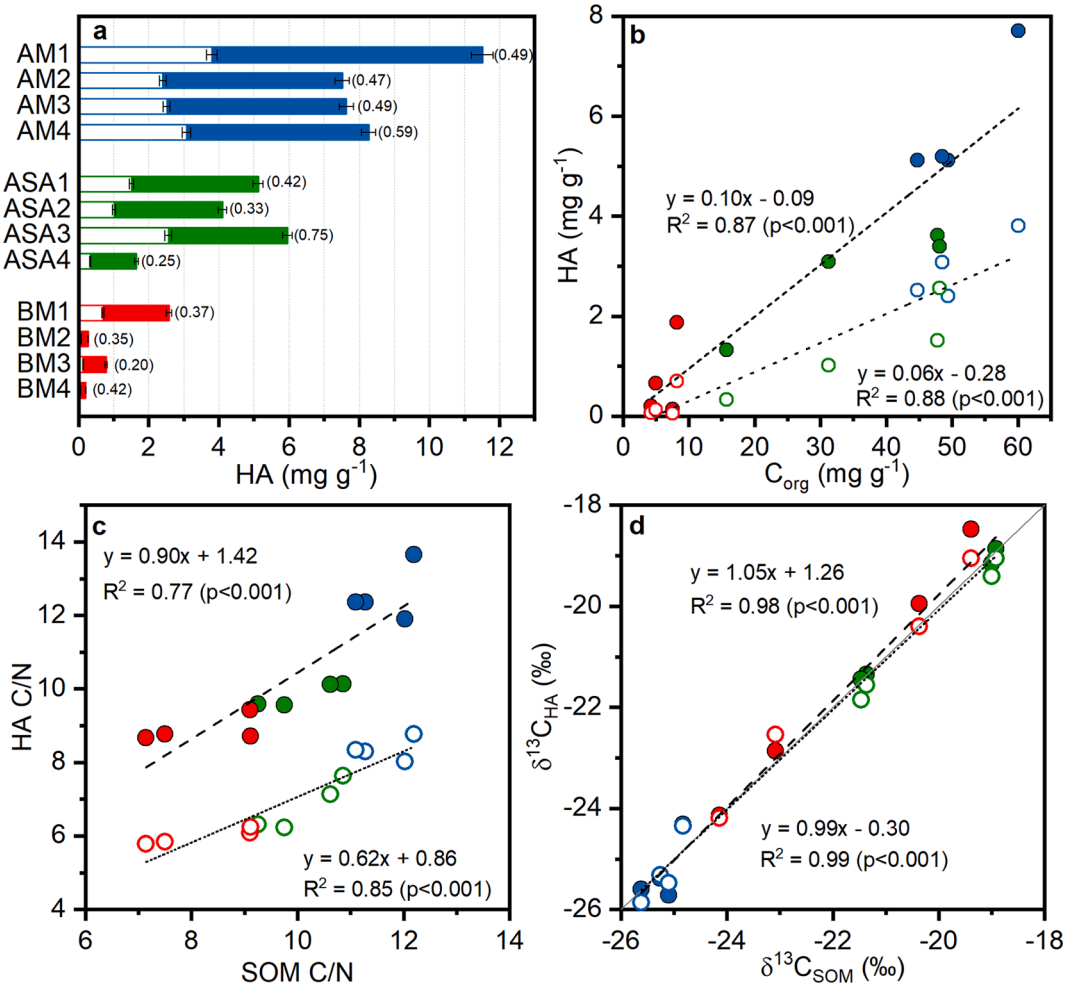

Fig. 2. (**a**) Free HA (FHA, empty bars) and bound HA (BHA, filled bars) content and FHA/BHA ratios (in parenthesis) in the soils of the three saltmarshes (from the innermost to the outermost: AM blue, ASA green, BM red). (**b**) Linear relationships between FHA (empty circles) and BHA (filled circles) contents and the corresponding soil C_{org} values. (**c**) Linear regression models of C/N ratios of FHA and BHA versus their corresponding SOM C/N values. (**d**) Linear regression models of $\delta^{13}C$ values of FHA and BHA versus their corresponding SOM $\delta^{13}C$ values. Grey diagonal is a 1:1 line.

3.2. HA quantification and composition

The proportions of C_{org} present in soil as either FHA or BHA are reported in Fig. 2a. Both fractions show a decreasing trend from the innermost part of the lagoon (AM saltmarsh, 2.95 ± 0.64 mg g^{-1} and 5.78 ± 1.29 mg g^{-1} for FHA and BHA, respectively) towards the barrier island (BM saltmarsh, 0.24 ± 0.31 mg g^{-1} and 0.72 ± 0.81 mg g^{-1} for FHA and BHA, respectively). However, in all soils, the amount of C_{org} in the BHA pool is larger than that in the FHA pool, with an overall mean FHA/BHA ratio of 0.43 ± 0.15. This result is due to the amounts of FHA and BHA which are strongly correlated with soil accumulation of C_{org} (R^2 = 0.88, $p < 0.001$ for FHA and R^2 = 0.87, $p < 0.001$ for BHA), although slope of the regression line is significantly steeper for BHA (Fig. 2b).

The C/N ratios of both FHA and BHA also exhibit a decreasing trend from the mainland towards the back-barrier saltmarsh, as observed for the whole SOM values (Fig. 2c). No significant differences in elemental C content are observed between the two fractions (mean value of 49.4 ± 2.8 % and 51.7 ± 2.2 % for FHA and BHA, respectively), whereas BHA contain less N than FHA (mean value of 7.2 ± 1.2 % and 5.1 ± 8.3 % for FHA and BHA, respectively) and the C/N ratios of BHA are, on average, about 50% higher than those of FHA from the same soil samples (Fig. 2c).

The $\delta^{13}C$ values of FHA and BHA strictly follow the trend shown by SOM and fall on the same linear regression model, close to a 1:1 relationship of $\delta^{13}C_{HA}$ versus $\delta^{13}C_{SOM}$, for both FHA and BHA (Fig. 2d).

3.3. UV–vis spectroscopic parameters

The specific absorbance of all HA (Fig. S6), decreases at longer wavelengths, exhibiting a typical behavior (MacCarthy and Rice, 1985). Spectra of FHA are characterized by an absorbance shoulder at 270–280 nm, related to the overlapping absorbance of unsaturated chromophores ($\pi - \pi^*$ electronic transitions, Chin et al., 1994; Peuravuori and Pihlaja, 1997), and a smaller shoulder at about 320 nm. Filip et al. (1988) observed similar spectral features in HA extracted from saltmarshes dominated by *Spartina alterniflora* and attributed these features to lignin structures, but in our case they were not limited to sites where *Spartina maritima* was the main cover. The same features were present, but less evident, in the spectra of BHA.

Specific UV absorbances at 254 nm ($SUVA_{254}$), commonly used to compare HA of different origin and as an index of aromaticity (Roccaro et al., 2015), are reported in Table 1. At all stations the $SUVA_{254}$ values of FHA and BHA are positively correlated ($R^2 = 0.89$, $p < 0.001$, inset in Fig. S6) and the average values of each saltmarsh decrease from the AM to the BM saltmarsh.

3.4. FTIR spectra of HA

Average FTIR spectra of FHA and BHA from each saltmarsh are reported in Fig. 3a, whereas single spectra are reported in Fig. S7. All FTIR spectra of FHA and BHA exhibit the typical HA bands (Senesi and Loffredo, 1999) and namely: a broad adsorption around 3280 cm^{-1} (H-bonded OH and N–H stretching), a composite band at 2700–3000 cm^{-1} comprising the twin peaks at 2920 and 2850 cm^{-1} (respectively asymmetric and symmetric aliphatic C–H stretching), 1720 cm^{-1} (C = O stretching of carboxyls), 1640–1630 cm^{-1} (C = C vibrations in aromatic rings, H-bonded C = O stretching of quinone and/or conjugated ketone and amide groups (amide I band), 1515 cm^{-1} (aromatic ring breathing, amide II band), 1400–1440 cm^{-1} (O–H deformation, CH_2 and CH_3 bending, C–O stretching of phenolic OH, antisymmetric stretching of aryl esters), 1250 cm^{-1} (C–O stretching and OH deformation of COOH, C–O stretching of aryl-esters). Absorption bands around 1150 cm^{-1} and 1030 cm^{-1} can be assigned to C-O and C–C stretching vibrations of pyranose rings in algal polysaccharides and to alcoholic C–O–H groups. The 1030 cm^{-1} band, increases continuously with the distance from the mainland in BHA, but reaches maximum intensity in FHA from the BM back-barrier saltmarsh soils. The relative intensities of these bands vary and display a somewhat regular trend for FHA. The aliphatic bands at 2700–3000 and 1400–1440 cm^{-1} are weaker in FHA and increase in strength from nearshore AM to the barrier island (BM). Besides, the 1720 cm^{-1} band of C = O stretching in COOH is more intense in the BHA extracted from the barrier island (BM), whereas the 1640 cm^{-1} band of the AM saltmarsh shifts to 1632 and 1628 cm^{-1} in FHA of the ASA and BM saltmarshes. This band and the 1514 cm^{-1} band, typically connected to amides, display a maximum intensity in FHA from the ASA saltmarsh. A more intense absorption in the region typical of CH_2 stretching vibrations (2700–3000 cm^{-1}) is displayed by BHA, indicating a stronger hydrophobic nature. At the same time, amide I and II bands are less pronounced in BHA. Apart from the HA extracted from the ASA saltmarsh, BHA do not seem to be affected by either the frequency and length of inundation or the vegetation type and display a much lower structural variability than FHA (Fig. S7).

3.5. ^{13}C NMr

Solid state ^{13}C NMR spectra (Fig. 3b) complement the structure assessment from FTIR. All ^{13}C NMR spectra exhibit the same peaks reported for HA extracted from other saltmarsh soils (Santín et al., 2008, 2009; Ferreira et al., 2013; Zhang et al., 2014). However, differences in peak intensities are observed among saltmarshes and for different types of HA.

In all samples, the alkyl C (0–45 ppm) region is the most abundant, displaying comparable values (range of 30.6–44.3 %) to those already

Table 1
Spectroscopic parameters from UV–vis and EPR spectroscopy of free HA (FHA) and bound (BHA) in the examined saltmarsh soils: specific UV absorbance at 254 nm ($SUVA_{254}$), semiquinone-type free radical (SFR) content, linewidth (ΔH) and spectroscopic splitting factor (*g*). Numbers in parenthesis represent standard deviations (n = 3).

Station	FHA				BHA			
	$SUVA_{254}$ L mg^{-1} cm^{-1}	SFR spins $g_{HA}^{-1} \times 10^{17}$	ΔH G	*g*	$SUVA_{254}$ L mg^{-1} cm^{-1}	SFR spins $g_{HA}^{-1} \times 10^{17}$	ΔH G	*g*
AM1	2.70 (0.13)	3.48 (0.18)	9.10	2.00487	3.21 (0.15)	4.05 (0.25)	7.19	2.00434
AM2	3.07 (0.09)	3.57 (0.16)	8.99	2.00486	4.05 (0.20)	4.60 (0.24)	7.12	2.00437
AM3	1.43 (0.06)	1.00 (0.07)	8.50	2.00443	2.02 (0.13)	2.49 (0.11)	7.12	2.00422
AM4	2.15 (0.11)	2.37 (0.09)	8.48	2.00424	2.55 (0.09)	2.83 (0.12)	6.91	2.00424
ASA1	0.85 (0.04)	0.68 (0.05)	8.53	2.00474	2.02 (0.10)	1.91 (0.09)	7.48	2.00428
ASA2	0.83 (0.04)	0.75 (0.04)	8.62	2.00462	1.71 (0.07)	1.75 (0.06)	7.51	2.0043
ASA3	2.38 (0.10)	3.23 (0.15)	9.52	2.00461	3.09 (0.13)	3.43 (0.18)	7.51	2.00475
ASA4	1.28 (0.07)	1.17 (0.09)	8.76	2.00482	2.37 (0.12)	2.18 (0.13)	6.58	2.00429
BM1	1.58 (0.07)	1.73 (0.07)	9.44	2.00480	2.78 (0.11)	3.67 (0.17)	7.60	2.00487
BM2	1.59 (0.06)	2.23 (0.12)	8.74	2.00463	2.74 (0.15)	3.45 (0.20)	7.20	2.00462
BM3	0.65 (0.04)	0.50 (0.07)	7.97	2.00482	1.58 (0.08)	3.06 (0.13)	7.19	2.0047
BM4	0.64 (0.05)	0.48 (0.03)	8.72	2.00470	1.49 (0.09)	2.12 (0.09)	6.92	2.0046

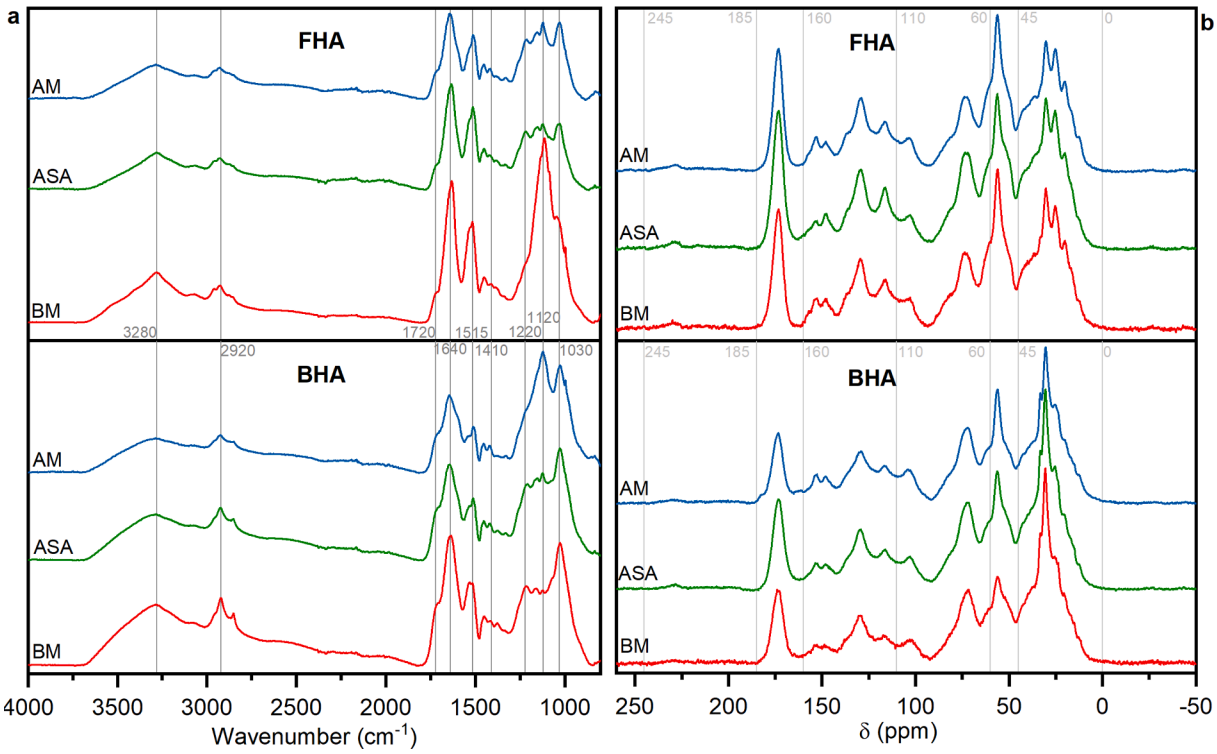

Fig. 3. Average FTIR (**a**) and ^{13}C NMR (**b**) spectra of free HA and bound HA extracted from the soils of the three saltmarshes (from the innermost to the outermost: AM, ASA and BM). Each spectrum was computationally obtained by averaging the individual spectra of the HA extracted in each saltmarsh.

reported for HA in similar environments (Santín et al., 2009; Ferreira et al., 2013). The contribution of alkyl C is larger in BHA than in FHA, due to the presence of a more intense peak at 30 ppm, typical of the internal methylene C in long alkyl chains (Preston, 1996). In FHA, the presence of two secondary peaks at 25 and 20 ppm, from short chain alkyl structures, such as methyl groups in hemicelluloses or peptide structures is also evident (Knicker, 2000). In BHA these peaks are present only as shoulders of the 30 ppm peak. Coherently with their larger N content, the signal at 55 pm reveals an important contribution of protein-like and methoxy compounds in FHA. The carbohydrate C groups (O-alkyl C) of FHA (73 and 102 ppm) show a decreasing trend in FHA from the AM to the BM saltmarsh, whereas in BHA the values are more homogeneous. In the aromatic region (110–160 ppm), the 115 and 130 ppm signals (attributed to lignin C, Kögel-Knabner, 2002) are related with the double signal in the range 145–155 ppm, which may be attributed to phenolic C in lignin structures. These signals are poorly defined in both the HA fractions of the BM saltmarsh, suggesting a relatively lower structural contribution of lignin and tannins. The well-defined signal at 173 ppm, attributed to carboxyl groups (like hemicelluloses and fatty acids; Kögel-Knabner, 1997), is more intense in FHA compared to BHA.

3.6. EPR

A representative EPR spectrum of both free and bound HA is reported in Fig. S8. Each spectrum shows the signal of the organic radicals present in the sample and the signal of the secondary standard. In all EPR spectra, the *g* value varied from 2.004 to 2.005, displaying typical values of oxygen-centered radical species such as semiquinones and methoxybenzenes (Cheshire and Senesi, 1998; Martin-Neto et al., 1998; Watanabe et al., 2005). Information associated to the relaxation time of free radical signals is provided by the linewidth (ΔH) values, that can be affected by structural aspects of HA molecules. No significant differences were found among the three saltmarshes, whereas in all samples the ΔH values of the FHA (average of 8.79 ± 0.45 G) are about 20 % higher than those of the corresponding BHA (7.22 ± 0.30 G, see Table 1). This result suggests that the radicals are better stabilized in BHA and radical species have a longer relaxation lifetime, indicated by smaller linewidth. The average SFR content of BHA (range 1.75–4.60 spins $g_{HA}^{-1} \times 10^{17}$) is coherent with this observation, being about 60 % larger than that of FHA (range 0.50–3.48 spins $g_{HA}^{-1} \times 10^{17}$) and displays lower variability within each saltmarsh (Fig. S9a). The largest contents are found in the BHA and FHA of the AM saltmarsh (2.60 ± 1.20 and 3.50 ± 1.00 spins $g_{HA}^{-1} \times 10^{17}$ for FHA and BHA, respectively), which is the sampling site nearest to the mainland. Similar values were measured in HA extracted from a Spanish salt marsh soil (Ferreira et al., 2013). In both fractions, the SFR content is highly related to the $SUVA_{254}$ (Fig. S9b) and therefore to the aromaticity of HA molecules ($R^2 = 0.95$, $p < 0.001$ for FHA and $R^2 = 0.73$, $p < 0.001$ for BHA). These results agree with those reported by Chen et al. (1977) and Martin-Neto et al. (1998), that showed that the SFR content increases with the degree of humification.

3.7. EDC of HA

At both acidic and neutral pH, the time course of the reaction of the HA with the radical $ABTS^{\bullet-}$ (followed monitoring the A_{734} over time, Fig. S10) is similar to the trends reported in the literature (Bravo et al., 2022; Walpen et al., 2020), being characterized by an initial steep decrease in absorbance followed by a slower exponential decline.

In all samples, the EDC_{fast} values obtained at pH 7.0 are higher (50–60 %) than those obtained at pH 4.8 (Fig. S11a). In fact, more redox active phenolic groups are dissociated at higher pH and, consequently, more prone to transfer electrons (Stone, 1987; Lee and von Gunten, 2010). At the same time, the molecular or supramolecular conformation of HA is more expanded, because of charge repulsion effects, thus electron transfer from reactive groups is favored (Hosse and Wilkinson, 2001). The EDC_{fast} values of FHA and BHA are positively correlated, both at acidic ($R^2 = 0.73$, $p < 0.001$) and neutral pH ($R^2 = 0.87$, $p < 0.001$) (Fig. S11b). In addition, BHA show higher EDC_{fast} values (about 20 %) compared to FHA, probably due to their higher molecular

complexity (Xiao et al., 2019) (Fig. 4a). The slow EDC component (EDC_{slow}) ranges between 0.95 and 1.11 $mmol_{e-}\ g_{HA}^{-1}$, with no significant differences among FHA and BHA or among HA from different sites.

Since fast processes are more relevant to support electron transfer for biological reactions occurring in soils, and considering the neutral pH of the soils examined in this study, the EDC_{fast} measured at pH 7.0 represents the best proxy to quantify the potential exhibited by HA to transfer electrons to other reducible soil components. The EDC_{fast} values of FHA (Fig. 4a) follow a decreasing trend moving from the AM saltmarsh (mean values of 0.77 ± 0.10 $mmol_{e-}\ g_{HA}^{-1}$) to the BM saltmarsh soils (mean value of 0.55 ± 0.07 $mmol_{e-}\ g_{HA}^{-1}$). HA from the ASA saltmarsh show intermediate values (mean value of 0.64 ± 0.13 $mmol_{e-}\ g_{HA}^{-1}$). BHA partly reflect the trend observed for FHA with HA from the AM soils showing the highest values (0.99 ± 0.13 $mmol_{e-}\ g_{HA}^{-1}$).

Klein et al. (2018) suggested that the EDC determination of HA with the ABTS decolorization assay should be carried out at acidic pH, in order to avoid errors associated with the decay of the radical at neutral pH and enable the reaction to proceed for 10 h in order to achieve a steady state. In this work, we measured EDC at pH 7 because kinetic analysis showed that the reaction occurs through two concomitant mechanisms: a fast reaction that achieves 95% completeness within 0.5 min and a slow reaction that requires hours to reach comparable near equilibrium conditions. Measurements were also performed at pH 4.8 to check whether this allowed a better reproducibility or resulted in better defined relationships with structural and environmental parameters. EDC measured at pH 4.8 and at pH 7 were highly correlated ($R^2 = 0.72$, $p < 0.001$).

4. Discussion

4.1. Geochemical signatures

Chemical properties of HA are well differentiated based on HA type (FHA vs. BHA), but also shaped by geographical gradients and organic inputs (autochthonous vs. allochthonous, terrestrial vs. marine). Site-specific factors alter the HA properties and challenge the comprehensive overview of the state of HA in this transitional environment. In order to gather together the data collected on soil and HA properties along the mainland-open sea geographical transect, results were further organized in heat maps, highlighting site or HA type (Fig. 5).

The heat map of soil and SOM characteristics (Fig. 5a) allows to visualize coherent geographical and morphological trends among and within the three saltmarshes examined in this study. For most characteristics, the effect of the saltmarsh location (e.g., distance from mainland) prevails over the effect of micromorphology which affects the hydroperiod and the local soil E_h. The E_h is the parameter that shows the lowest connection with other soil characteristics, possibly because of the many independent factors that concur to its determination (e.g., including vegetation type).

The fraction of SOM stabilized in the soils as HA (FHA + BHA) is, on average, only 8.1 % of the C_{org} in AM saltmarsh and C sequestration in the form of HA is even lower in soils of ASA and BM saltmarshes (5.3 and 4.0 %, respectively). Their importance in this transitional environment, where $CaCO_3$ saturated freshwater inputs inhibit transport of dissolved HA from the mainland, lies more in their role in geochemical processes than in their contribution to C sequestration. The heat map (Fig. 5a)

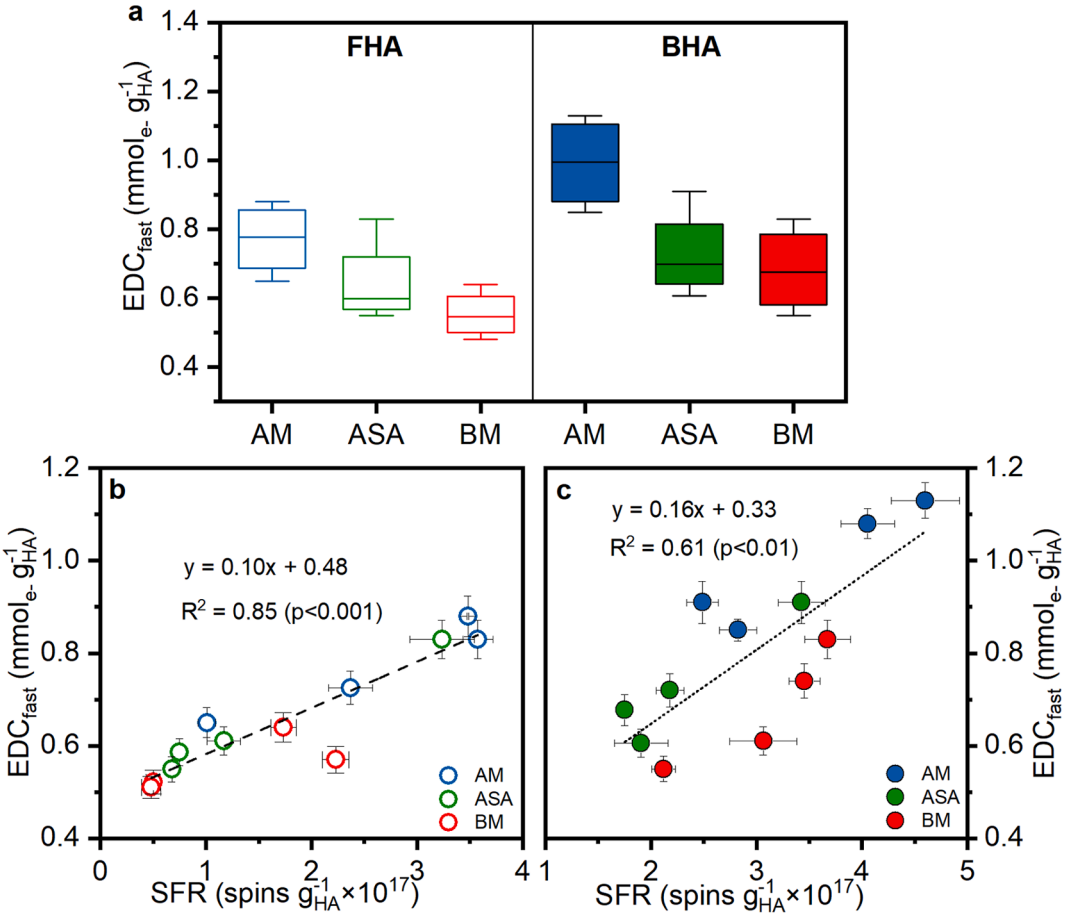

Fig. 4. (**a**) Box plots of the fast electron donating capacities (EDC_{fast}) measured at pH 7.0 of free HA (FHA) and bound HA (BHA) extracted from the three different saltmarshes (from the innermost to the outermost: AM, ASA and BM). The line within the box marks the median and the boundaries of the box indicate the 25th and 75th percentiles. (**b, c**) Linear correlations between EDC_{fast} and semiquinone-type free radicals (SFR) in FHA (empty circles) and BHA (filled circles).

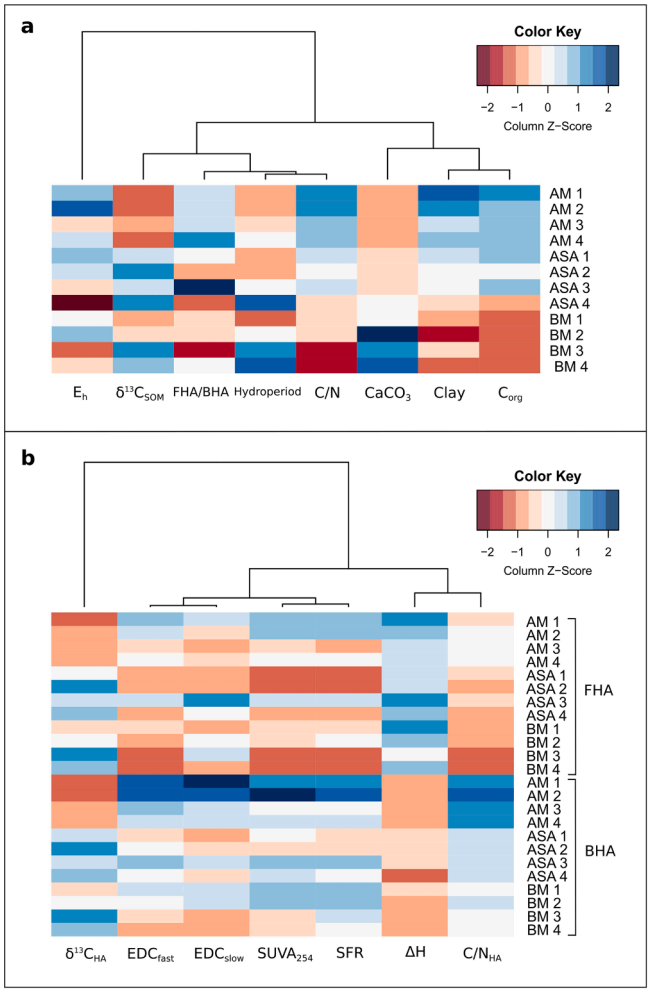

Fig. 5. Heat maps of (**a**) soil properties and (**b**) free HA (FHA) and bound HA (BHA) characteristics in the different soils of the three saltmarshes (from the innermost to the outermost: AM, ASA and BM). Variables were normalized using the Z-score function. Selected soil variables are: soil E_h, carbon stable isotope composition ($\delta^{13}C_{SOM}$), FHA/BHA ratio, average hydroperiod, soil C/N ratio, carbonate content ($CaCO_3$), clay content and total organic carbon (C_{org}). Selected HA features are: carbon stable isotope composition of HA ($\delta^{13}C_{HA}$), EDC_{fast}, EDC_{slow}, specific UV absorbance at 254 nm ($SUVA_{254}$), semiquinone-free radical (SFR) content, linewidth (ΔH) and C/N ratio of HA.

highlights that FHA contribution to the HA pool (based on FHA/BHA ratio) is related to soil hydroperiod and SOM C/N ratios. In fact, reducing conditions in flooded soils hinder humification and increase the relative abundance of fulvic acids (Sheudzhen and Gutorova, 2020). Moreover, despite most of HA properties (e.g., EDC_{fast} values) seem related to the combined effect of HA type and sampling site location (Fig. 5b), the analysis highlights that the two HA fractions are well differentiated based on some specific chemical characteristics, in particular their C/N ratios, that are highly dependent on HA nature. The low energy depositional environment seems to be an important factor for accumulation of HA in these soils, coherently with the fact that C_{org} accumulation is also governed by their clay content (Fig. S12).

The C/N ratios of both FHA and BHA decrease significantly from the innermost to the outermost sector of the lagoon, similarly to the trend observed in sediments from the same lagoon (Bravo et al., 2020). The lowest C/N ratios found in FHA from soils nearest to the open sea may reflect a strong input from algal materials stranded by waves and storms. The C/N ratios of BHA are higher than those of FHA extracted from the same soils, but contrary to what occurs in sediments, chemical features suggest a more pronounced local origin. During accretion of saltmarshes, HA formed in terrestrial soils and bound to fine silt and clay particles, transported in suspension by tidal currents, may deposit on saltmarshes particularly during spring tides, when both the input from rivers and the submergence time culminate (Zhou et al., 2006). Allochthonous BHA of terrestrial origin may partly contribute to differentiate HA structures in these soils, as they do in sediments. However, in soils, *in situ* humification and fractionation caused by higher hydrophobicity of BHA is likely to provide a much stronger contribution (Ferronato et al., 2019). This is confirmed by $SUVA_{254}$ values, which are higher for BHA (Table 1). At the same time, C/N values tend to increase linearly with the mean height above sea level in the transition from the mainland to the open sea, both in SOM and in FHA, whereas the trend is less significant for BHA.

Overall, the $SUVA_{254}$ values are significantly lower than those previously found in sediments of the same lagoon (Bravo et al., 2020), thus indicating a lower aromatic character of saltmarsh HA. This is opposite to the expectations based on *in situ* C inputs which infers a lower aromaticity due to contribution from non-vascular plants (algae), but coherent with the lowest deposition of suspended allochthonous organic materials of terrestrial origin on emerged soils.

Unlike sediments, soil HA reflect more strongly the contributions from the halophile vegetation inhabiting the saltmarsh and their characteristic depend on the elevation of the soil above sea level. This is more evident in FHA, whereas BHA also show evidence of a substantial contribution from terrestrial sedimentary materials. In general, our results point to a compositional variability along the mainland-sea transect represented by the three saltmarshes, which is consistent with previous results obtained from lagoon sediments (Bravo et al. 2020).

The ^{13}C NMR spectra show that BHA display stronger signals in the aliphatic region (0–110 ppm) with a particular intense signal at about 30 ppm, which can be attributed to C in methylene groups. This lowers the Arom/Alkyl ratios of BHA. Conversely, carboxyl groups are more abundant in FHA and N-alkyl/O-alkyl and aromatic-C/alkyl-C ratios decrease from AM towards BM saltmarshes. Similarly, methoxyl groups in FHA decrease with distance from the mainland.

4.2. *EDC of HA*

The reaction between HA and the radical $ABTS^{\bullet-}$ exhibits a biphasic kinetics driven by two concomitant mechanisms (Fig. S10), consisting of a fast and a slow electron transfer process (Bravo et al. 2022). Application of the bi-phasic model to the time trend of the reaction with $ABTS^{\bullet-}$ resulted in a very good fitting of experimental data for all samples. Besides, it revealed that the slow reaction mechanism does not differentiate the HA, but is either a contribution from a highly conserved feature or artifactually produced by auto-regeneration of ABTS radicals (Osman et al., 2006). A similar non-equilibrium transfer reaction trend was also observed for some polyphenols and ascribed to reproduction of reducible OH moieties by oxidative polymerization (Hotta et al., 2002).

On the contrary, the millimoles of electrons transferred per gram of HA through the fast reaction decreases from the innermost to the outermost saltmarsh soils and, although the difference between FHA and BHA is not significant, the EDC_{fast} displays a significant difference between AM and BM HA in both fractions. The electrons transferred during the first 0.5 min represent from 35 to 50% of the total amount transferred in 12 h.

Radicals in HA are thought to be very reactive in redox reactions (Senesi et al., 1977; Oniki and Takahama, 1994) and actually the EDC_{fast} of HA showed a linear correlation with SFR concentration (Fig. 4b, c). The EDC also correlated strongly ($R^2 = 0.80$, $p < 0.01$) with the average area of aromatic C signals measured by ^{13}C NMR of BHA in the three saltmarshes, whereas a less strong relationship was found with FHA. Considering that absorption at 254 nm is not only caused by carboxy phenols (Baes and Bloom, 1990), but also by aromatic amino acids, it is possible that these groups may additionally contribute to the electron donating capacity of HA.

4.3. Environmental implications of EDC measurements

In principle, the EDC of HA should directly reflect the intensity of reduction in soil, however in this work no relationship was found between the fast or the slow EDC of HA and soil Eh, neither at pH 4.8 nor at pH 7. This indicates that other factors concur in determining the state of reduction of HA: for instance, HA in low lying soils may be fully reduced, but if their maximum electron accepting capacity is low (low density of redox active moieties per gram of HA) they could have reached full reduction at higher Eh values and not be able to accept more electrons. This would limit their capacity to fully reflect the redox state of the soil. Another factor might be the presence/contact with electron accepting mineral soil components, like iron oxides. HA are known to act as electron shuttles and their EDC therefore reflects not only the intensity of reduction, but also the ease with which electrons are passed onto iron oxides, which may depend on spatial constraints (e.g. inequalities in distribution caused by the presence of iron depletions and iron crusts).

The chemical speciation and mobility of redox-sensitive elements (like Fe, Mn, As, Hg) is influenced by redox processes in which HA are involved (Bauer and Kappler, 2009). These processes of HA are ecologically important in tidal environments, where soils are subject to recurring 12 h cycles of flooding and drainage (Lee et al., 2019). Under anaerobic conditions, the reduction of HA facilitates the oxidation of organic substrates trough anaerobic respiration, especially if regeneration of the original redox state is achieved by shuttling electrons to Fe (III) and Mn(IV) oxides. HA can mediate the reduction of metal oxides that cannot be directly achieved by bacteria (Zachara et al., 1998) and do not necessarily have to be abundant to play a key role as electron acceptors.

The hydroperiod varies greatly within soils of the same saltmarsh, depending on soil elevation, and affects the soil redox potential. Redox chemistry of Fe and Mn, and accumulation/uptake of potentially toxic metals (PTM) in saltmarsh plants are therefore affected. Here, HA can compete in the root iron plaque formation, by reducing Fe(III) back to Fe (II).

In the Marano Lagoon, saltmarshes and bottom sediments are widely contaminated by mercury (Hg) (Acquavita et al., 2012), displaying values higher than the regional background (0.13 ± 0.04 mg kg^{-1}, Covelli et al., 2006). In the surface soil horizon of a saltmarsh closed to the AM site, Covelli et al. (2017) reported Hg contents between 2.57 and 4.70 mg kg^{-1}. The mobility of Hg in tidal environments depends on several biogeochemical processes, in which HA play an important role (Ravichandran, 2004). In fact, HA have been demonstrated to be involved in both complexation (Chiasson-Gould et al., 2014) and reduction (Jiang et al., 2014) of Hg. Alberts et al. (1974) demonstrated that free radicals in HA are directly involved in Hg reduction. Consequently, the EDC of HA could be a key factor governing the fate of Hg in polluted soils and sediments. Jiang et al. (2014) reported that, in addition to temperature and light exposure, HA significantly increase Hg(0) production and SOM with higher aromatic character was found to display higher EDC values and more rapid kinetics towards Hg(II) reduction (Jiang et al. 2020). Nevertheless, globally rising temperatures are expected to alter the ability of HA to participate in critical redox processes by decreasing their EDC (LaCroix et al., 2021), thus reducing HA ability to contain Hg toxicity in coastal soils.

5. Conclusions

The exhaustive characterization of SOM and HA in twelve tidal soils in three saltmarshes with different sedimentary and transformation processes shows that geographical location and elevation are main players influencing the chemical and structural characteristics of SOM. Humic acids faithfully reflect the composition of SOM, but display peculiar features that confirm their distinctive nature.

The results obtained in this work confirmed the importance of aromatic structure of HA and showed that bound HA (BHA) present higher EDC values compared to free HA (FHA). However, the actual measured fast transfer component of EDC of both FHA and BHA is largely related to the geochemical characteristics of soils (i.e. soil texture and terrestrial/marine inputs), which is therefore relevant to understand the redox processes in transitional environments.

Declaration of Competing Interest

The authors declare that they have no known competing financial interests or personal relationships that could have appeared to influence the work reported in this paper.

Acknowledgements

C. Bravo acknowledges the financial support provided by Research Traineeship (TRA 2019-2) from the International Humic Substances Society, to stay at Embrapa Instrumentação Research Center, São Carlos/SP, Brazil. This research was partly supported by the São Paulo Research Foundation (FAPESP Grant no. 2018/08738-2 to C. Millo).

Appendix A. Supplementary data

Supplementary data to this article can be found online at https://doi.org/10.1016/j.geoderma.2022.115872.

References

Acquavita, A., Covelli, S., Emili, A., Berto, D., Faganeli, J., Giani, M., Horvat, M., Koron, N., Rampazzo, F., 2012. Mercury in the sediments of the Marano and Grado Lagoon (northern Adriatic Sea): sources, distribution and speciation. Estuar. Coast. Shelf S. 113, 20–31. https://doi.org/10.1016/j.ecss.2012.02.012.

Aeschbacher, M., Graf, C., Schwarzenbach, R.P., Sander, M., 2012. Antioxidant properties of humic substances. Environ. Sci. Technol. 46, 4916–4925. https://doi.org/10.1021/es300039h.

Alberts, J.J., Schindler, J.E., Miller, R.W., Nutter, D.E., 1974. Elemental mercury evolution mediated by humic acids. Science 184 (4139), 895–897.

Baes, A.U., Bloom, P.R., 1990. Fulvic acid ultraviolet-visible spectra: influence of solvent and pH. Soil Sci. Soc. Am. J. 54, 1248–1254. https://doi.org/10.2136/sssaj1990.03615995005400050008x.

Bauer, I., Kappler, A., 2009. Rates and extent of reduction of Fe(III) compounds and O2 by humic substances. Environ. Sci. Technol. 43, 4902–4908. https://doi.org/10.1021/es900179s.

Bravo, C., De Nobili, M., Gambi, A., Martin-Neto, L., Nascimento, O.R., Toniolo, R., 2022. Kinetics of electron transfer reactions by humic substances: Implications for their biogeochemical roles and determination of their electron donating capacity. Chemosphere 286, 131755. https://doi.org/10.1016/j.chemosphere.2021.131755.

Bravo, C., Millo, C., Covelli, S., Contin, M., De Nobili, M., 2020. Terrestrial-marine continuum of sedimentary natural organic matter in a mid-latitude estuarine system. J. Soils Sediments 20, 1074–1086. https://doi.org/10.1007/s11368-019-02457-6.

Bouyoucos, G.J., 1962. Hydrometer method improved for making particle size analyses of soils. Agron. J. 54, 464–465. https://doi.org/10.2134/agronj1962.00021962005400050028x.

Chen, Y., Senesi, N., Schnitzer, M., 1977. Information provided on humic substances by E4/E6 ratios. Soil Sc. Soc. Am. J. 41, 352–358. https://doi.org/10.2136/sssaj1977.03615995004100020037x.

Cheshire, M.V., Senesi, N., 1998. Electron spin resonance spectroscopy of organic and mineral soil particles. In: Huang, P.M., Senesi, N., Buffle, J. (Eds.), Structure and surface reactions of soil particles. Wiley, Chichester, UK, pp. 325–374.

Chiasson-Gould, S.A., Blais, J.M., Poulain, A.J., 2014. Dissolved organic matter kinetically controls mercury bioavailability to bacteria. Environ. Sci. Technol. 48, 3153–3161. https://doi.org/10.1021/es4038484.

Chin, Y.P., Aiken, G., O'Loughlin, E., 1994. Molecular weight, polydispersity, and spectroscopic properties of aquatic humic substances. Environ. Sci. Technol. 28, 1853–1858. https://doi.org/10.1021/es00060a015.

Chmura, G.L., Anisfeld, S.C., Cahoon, D.R., Lynch, J.C., 2003. Global carbon sequestration in tidal, saline wetland soils. Global Biogeochem. Cy. 17 (4), n/a–n/a.

Covelli, S., Fontolan, G., Faganeli, J., Ogrinc, N., 2006. Antrophogenic markers in the Holocene stratigraphic sequence of the Gulf of Trieste (northern Adriatic Sea). Mar. Geol. 230, 29–51. https://doi.org/10.1016/j.margeo.2006.03.013.

Covelli, S., Petranich, E., Langone, L., Emili, A., Acquavita, A., 2017. Historical sedimentary trends of mercury and other trace elements from two saltmarshes of the Marano and Grado lagoon (northern Adriatic Sea). J. Soils Sediments 17, 1972–1985. https://doi.org/10.1007/s11368-016-1618-8.

De Nobili, M., Contin, M., Mahieu, N., Randall, E.W., Brookes, P.C., 2008. Assessment of chemical and biochemical stabilization of organic C in soils from the long-term experiments at Rothamsted (UK). Waste Manage. 28, 723–733. https://doi.org/10.1016/j.wasman.2007.09.025.

Duarte, C.M., Delgado-Huertas, A., Anton, A., Carrillo-de-Albornoz, P., López-Sandoval, D.C., Agustí, S., Almahasheer, H., Marbá, N., Hendriks, I.E., Krause-Jensen, D., Garcias-Bonet, N., 2018. Stable isotope (δ13C, δ15N, δ18O, δD) composition and nutrient concentration of Red Sea primary producers. Frontiers in Marine Science 5. https://doi.org/10.3389/fmars.2018.00298.

Ferreira, F.P., Vidal-Torrado, P., Otero, X.L., Buurman, P., Martin-Neto, L., Boluda, R., Macias, F., 2013. Chemical and spectroscopic characteristics of humic acids in marshes from the Iberian Peninsula. J. Soils Sediments 13, 253–264. https://doi.org/10.1007/s11368-012-0607-9.

Ferronato, C., Marinari, S., Francioso, O., Bello, D., Trasar-Cepeda, C., Antisari, L.V., 2019. Effect of waterlogging on soil biochemical properties and organic matter quality in different salt marsh systems. Geoderma 338, 302–312. https://doi.org/10.1016/j.geoderma.2018.12.019.

Filip, Z., Alberts, J.J., Cheshire, M.V., Goodman, B.A., Bacon, J.R., 1988. Comparison of salt marsh humic acid with humic-like substances from the indigenous plant species Spartina alterniflora (Loisel). Sci. Total Environ. 71, 157–172. https://doi.org/10.1016/0048-9697(88)90164-7.

Fontolan, G., Pillon, S., Bezzi, A., Villalta, R., Lipizer, M., Triches, A., D'Aietti, A., 2012. Human impact and the historical transformation of saltmarshes in the Marano and Grado Lagoon, northern Adriatic Sea. Estuar. Coast. Shelf Sci. 113, 41–56. https://doi.org/10.1016/j.ecss.2012.02.007.

Hosse, M., Wilkinson, K.J., 2001. Determination of electrophoretic mobilities and hydrodynamic radii of three humic substances as function of pH and ionic strength. Environ. Sci. Technol. 35, 4301–4306. https://doi.org/10.1021/es010038r.

Hotta, H., Nagano, S., Ueda, M., Tsujino, Y., Koyama, J., Osakai, T., 2002. Higher radical scavenging activities of polyphenolic antioxidants can be ascribed to chemical reaction following their oxidation. Biochim. Biophys. Acta 1572, 123–132. https://doi.org/10.1016/S0304-4165(02)00285-4.

Jiang, T., Kaal, J., Liu, J., Liang, J., Zhang, Y., Wang, D., 2020. Linking the electron donation capacity to the molecular composition of soil dissolved organic matter from the Three Gorges Reservoir areas. China. J. Environ. Sciences 90, 146–156. https://doi.org/10.1016/j.jes.2019.11.007.

Jiang, T., Wei, S.-Q., Flanagan, D.C., Li, M.-J., Li, X.-M., Wang, Q., Luo, C., 2014. Effect of abiotic factors on the mercury reduction process by humic acids in aqueous systems. Pedosphere 24 (1), 125–136.

Kappler, A., Haderlein, S.B., 2003. Natural organic matter as reductant for chlorinated aliphatic pollutants. Environ. Sci. Technol. 37, 2714–2719. https://doi.org/10.1021/es0201808.

Keller, J.K., Weisenhorn, P.B., Megonigal, J.P., 2009. Humic acids as electron acceptors in wetland decomposition. Soil Biol. Biochem. 41, 1518–1522. https://doi.org/10.1016/j.soilbio.2009.04.008.

Klein, O.I., Kulikova, N.A., Filionov, I.S., Koroleva, O.V., Konstantinov, A.I., 2018. Long-term kinetics study and quantitative characterization of the antioxidant capacities of humic and humic-like substances. J. Soils Sediments 18, 1355–1364. https://doi.org/10.1007/s11368-016-1538-7.

Klüpflel, L., Piepenbrock, A., Kappler, A., Sander, M., 2014. Humic substances as fully regenerable electron acceptors in recurrently anoxic environments. Nat. Geosci. 7, 195–200. https://doi.org/10.1038/ngeo2084.

Knicker, H., Lüdemann, H.D., 1995. N-15 and C-13 CPMAS and solution NMR studies of N-15 enriched plant material during 600 days of microbial degradation. Org. Geochem. 23, 329–341. https://doi.org/10.1016/0146-6380(95)00007-2.

Knicker, H., 2000. Biogenic nitrogen in soils as revealed by solid-state carbon-13 and nitrogen-15 nuclear magnetic resonance spectroscopy. J. Environ. Qual. 29, 715–723. https://doi.org/10.2134/jeq2000.00472425002900030005x.

Kögel-Knabner, I., 1997. 13C and 15N NMR spectroscopy as a tool in soil organic matter studies. Geoderma 80, 243–270. https://doi.org/10.1016/S0016-7061(97)00055-4.

Kögel-Knabner, I., 2002. The macromolecular organic composition of plant and microbial residues as inputs to soil organic matter. Soil Biol. Biochem. 34, 139–162. https://doi.org/10.1016/S0038-0717(01)00158-4.

LaCroix, R.E., Walpen, N., Sander, M., Tfaily, M.M., Blanchard, J.L., Keiluweit, M., 2021. Long-Term Warming Decreases Redox Capacity of Soil Organic Matter. Environ. Sci. Technol. Lett. 8, 92–97. https://doi.org/10.1021/acs.estlett.0c00748.

Lee, S., Roh, Y., Koh, D.C., 2019. Oxidation and reduction of redox-sensitive elements in the presence of humic substances in subsurface environments: A review. Chemosphere 220, 86–97. https://doi.org/10.1016/j.chemosphere.2018.11.143.

Lee, Y., von Gunten, U., 2010. Oxidative transformation of micropollutants during municipal wastewater treatment: comparison of kinetic aspects of selective (chlorine, chlorine dioxide, ferrate VI, and ozone) and non-selective oxidants (hydroxyl radical). Water Res. 44, 555–566. https://doi.org/10.1016/j.watres.2009.11.045.

Lovley, D.R., Coates, J.D., Blunt-Harris, E.L., Phillips, E.J.P., Woodward, J.C., 1996. Humic substances as electron acceptors for microbial respiration. Nature 382, 445–448. https://doi.org/10.1038/382445a0.

MacCarthy, P., Rice, J., 1985. Spectroscopic methods (other than NMR) for determining functionality in humic substances. In: Aiken, G.R., McKnight, D.M., Wershaw, R.L., MacCarthy, P. (Eds.), Humic substances in soil, sediment and water. John Wiley & Sons, New York, pp. 527–559.

Martin-Neto, L., Rosell, R., Sposito, G., 1998. Correlation of spectroscopic indicators of humification with mean annual rainfall along a temperate grassland climosequence. Geoderma 81, 305–311. https://doi.org/10.1016/S0016-7061(97)00089-X.

Martin-Neto, L., Traghetta, D.G., Vaz, C.M.P., Crestana, S., Sposito, G., 2001. On the interaction mechanisms of atrazine and hydroxyatrazine with humic substances. J. Environ. Qual. 30, 520–525. https://doi.org/10.2134/jeq2001.302520x.

Miller, J.C., Miller, J.N., 2010. Statistics and chemometrics for analytical chemistry, 6th ed. Pearson, Harlow.

Mitsch, W., Hernandez, M., 2013. Landscape and climate change threats to wetlands of North and Central America. Aquat. Sci. 75, 133–149. https://doi.org/10.1007/s00027-012-0262-7.

Nieuwenhuize, J., Maas, Y.E.M., Middelburg, J.J., 1994. Rapid analysis of organic carbon and nitrogen in particulate materials. Mar. Chem. 45, 217–224. https://doi.org/10.1016/0304-4203(94)90005-1.

Nurmi, J.T., Tratnyek, P.G., 2002. Electrochemical properties of natural organic matter (NOM), fractions of NOM, and model biogeochemical electron shuttles. Environ. Sci. Technol. 36, 617–624. https://doi.org/10.1021/es0110731.

Olk, D.C., 2006. A chemical fractionation for structure–function relations of soil organic matter in nutrient cycling. Soil Sci. Soc. Am. J. 70, 1013–1022. https://doi.org/10.2136/sssaj2005.0108.

Olk, D.C., Bloom, P.R., Perdue, E.M., McKnight, D.M., Chen, Y., Farenhorst, A., Senesi, N., Chin, Y.P., Schmitt-Kopplin, P., Hertkorn, N., Harir, M., 2019. Environmental and agricultural relevance of humic fractions extracted by alkali from soils and natural waters. J. Environ. Qual. 48, 217–232. https://doi.org/10.2134/jeq2019.02.0041.

Oniki, T., Takahama, U., 1994. Effects of reaction time, chemical reduction, and oxidation on esr in aqueous solutions of humic acids. Soil Sci. 158, 204–210. https://doi.org/10.1097/00010694-199409000-00006.

Osman, A., Wong, K., Fernyhough, A., 2006. ABTS radical-driven oxidation of polyphenols. Isolation and structural elucidation of covalent adducts. Biochem. Biophys. Res. Commun. 346, 321–329. https://doi.org/10.1016/j.bbrc.2006.05.118.

Pellegrini, E., Contin, M., Vittori Antisari, L., Ferronato, C., De Nobili, M., 2019. Soil organic carbon and carbonates are binding phases for simultaneously extractable metals in calcareous saltmarsh soils. Environ. Toxicol. Chem. 38, 2688–2697. https://doi.org/10.1002/etc.4590.

Peuravuori, J., Pihlaja, K., 1997. Molecular size distribution and spectroscopic properties of aquatic humic substances. Anal. Chim. Acta 337, 133–149. https://doi.org/10.1016/S0003-2670(96)00412-6.

Preston, C.M., 1996. Applications of NMR to soil organic matter analysis: history and prospects. Soil Sci 161, 144–166. https://doi.org/10.1097/00010694-199603000-00002.

Rabenhorst, M.C., Needelman, B.A., 2016. Soils of tidal wetlands. In: Vepraskas, M.J., Craft, C.B. (Eds.), Wetland Soils. Genesis, Hydrology, Landscapes and Classification. CRC Press, Boca Raton, pp. 365–376.

Ratasuk, N., Nanny, M.A., 2007. Characterization and quantification of reversible redox sites in humic substances. Environ. Sci. Technol. 41, 7844–7850. https://doi.org/10.1021/es071389u.

Ravichandran, M., 2004. Interactions between mercury and dissolved organic matter – a review. Chemosphere 55, 319–331. https://doi.org/10.1016/j.chemosphere.2003.11.011.

Roccaro, P., Yan, M., Korshin, G.V., 2015. Use of log-transformed absorbance spectra for online monitoring of the reactivity of natural organic matter. Water Res. 84, 136–143. https://doi.org/10.1016/j.watres.2015.07.029.

Santín, C., González-Pérez, M., Otero, X.L., Vidal-Torrado, P., Macías, F., Álvarez, M.Á., 2008. Characterization of humic substances in salt marsh soils under sea rush (*Juncus maritimus*). Estuar. Coast. Shelf Sci. 79, 541–548. https://doi.org/10.1016/j.ecss.2008.05.007.

Santín, C., González-Pérez, M., Otero, X.L., Álvarez, M.Á., Macías, F., 2009. Humic substances in estuarine soils colonized by *Spartina maritima*. Estuar. Coast. Shelf Sci. 81, 481–490. https://doi.org/10.1016/j.ecss.2008.12.013.

Senesi, N., Chen, Y., Schnitzer, M., 1977. The role of free radicals in the oxidation and reduction of fulvic acid. Soil Biol. Biochem. 9, 397–403. https://doi.org/10.1016/0038-0717(77)90018-9.

Senesi, N., Loffredo, E., 1999. The cemistry of soil organic matter. In: Sparks, S.L. (Ed.), Soil physical chemistry, 2nd ed. CRC Press, Boca Raton, pp. 239–370.

Senesi, N., Steelink, C., 1989. Application of ESR spectroscopy to the study of humic substances. In: Hayes, M.H.B., et al. (Eds.), Humic substances II: In search of structure. Wiley, New York, pp. 373–408.

Sheudzhen, A.K., Gutorova, O.A., 2020. State of Humus in Soils under Rice Cultivation. In: IOP Conference Series: Materials Science and Engineering, 941 (1). IOP Publishing.

Steinberg, C., 2013. Humic substances as geochemical determinants. In: Ecology of Humic Substances in Freshwaters. Springer, Berlin, pp. 65–115.

Stevenson, F.J., 1982. Extraction, fraction and general chemical composition of soil organic matter. In: Humus Chemistry, Genesis, Composition, Reactions. John Wiley and Sons.

Stone, A.T., 1987. Reductive dissolution of manganese (iii/iv) oxides by substituted phenols. Environ. Sci. Technol. 21, 979–988. https://doi.org/10.1021/es50001a011.

Struyk, Z., Sposito, G., 2001. Redox properties of standard humic acids. Geoderma 102, 329–346. https://doi.org/10.1016/S0016-7061(01)00040-4.

Valenzuela, E.I., Avendaño, K.A., Balagurusamy, N., Arriaga, S., Nieto-Delgado, C., Thalasso, F., Cervantes, F.J., 2019. Electron shuttling mediated by humic substances fuels anaerobic methane oxidation and carbon burial in wetland sediments. Sci. Tot. Environ. 650, 2674–2684. https://doi.org/10.1016/j.scitotenv.2018.09.388.

Voelker, B., Morel, F.M.M., Sulzberger, B., 1997. Iron redox cycling in surface waters: Effects of humic substances and light. Environ. Sci. Technol. 31, 1004–1011. https://doi.org/10.1021/es9604018.

Walpen, N., Houska, J., Salhi, E., Sander, M., Von Gunten, U., 2020. Quantification of the electron donating capacity and UV absorbance of dissolved organic matter during ozonation of secondary wastewater effluent by an assay and an automated analyzer. Water Research 185, 116235. https://doi.org/10.1016/j.watres.2020.116235.

Watanabe, A., McPhail, D.B., Maie, N., Kawasaki, S., Anderson, H.A., Cheshire, M.V., 2005. Electron spin resonance characteristics of humic acids from a wide range of

soil types. Org. Geochem. 36, 981–990. https://doi.org/10.1016/j.orggeochem.2005.03.002.

Xia, S., Song, Z., Li, Q., Guo, L., Yu, C., Singh, B.P., Fu, X., Chen, C., Wang, Y., Wang, H., 2021. Distribution, sources, and decomposition of soil organic matter along a salinity gradient in estuarine wetlands characterized by C: N ratio, δ13C-δ15N, and lignin biomarker. Glob. Change Biol. 27 (2), 417–434.

Xiao, X., Xi, B.D., He, X.S., Zhang, H., Li, D., Zhao, X.Y., Zhang, X.H., 2019. Hydrophobicity-dependent electron transfer capacities of dissolved organic matter derived from chicken manure compost. Chemosphere 222, 757–765. https://doi.org/10.1016/j.chemosphere.2019.01.173.

Zachara, J.M., Fredrickson, J.K., Li, S.M., Kennedy, D.W., Smith, S., Gassman, P.L., 1998. Bacterial reduction of crystalline Fe^{3+} oxides in single phase suspensions and subsurface materials. Am. Mineral. 83, 1426–1443. https://doi.org/10.2138/am-1998-11-1232.

Zhang, Y., Du, J., Zhao, X., Wu, W., Peng, B., Zhang, J., 2014. A multi-proxy study of sedimentary humic substances in the salt marsh of the Changjiang Estuary. China. Estuar. Coast. Shelf Sci. 151, 295–301. https://doi.org/10.1016/j.ecss.2014.10.007.

Zhou, J., Wu, Y., Zhang, J., Kang, Q., Liu, Z., 2006. Carbon and nitrogen composition and stable isotope as potential indicators of source and fate of organic matter in the salt marsh of the Changjiang Estuary, China. Chemosphere 65, 310–317. https://doi.org/10.1016/j.chemosphere.2006.02.026.